

ESTIMATION OF HIGH TEMPERATURE FATIGUE
LIFETIME OF SUS304 STEEL WITH AN ENERGY
PARAMETER IN THE CRITICAL PLANE

TADEUSZ ŁAGODA

EWALD MACHA

Technical University of Opole

e-mail: tlag@po.opole.pl; emac@po.opole.pl

MASAO SAKANE

Ritsumeikan University, Nojihigashi Kusatsu-shi Shiga, Japan

The paper studies the application of the energy parameter, a sum of elastic and plastic strain energy densities in the critical plane, for the correlation of two series of proportional biaxial low-cycle lives using SUS304 stainless steel at elevated temperature. The first data used thin-walled cylinder specimens subjected to 7 proportional strain paths of combined tension-torsion and the other used cruciform specimens subjected to 5 proportional strain paths of biaxial tension-compression. These tests were done at the temperature of 923 K. The normal total strain energy density in the plane with the maximum damage was a suitable parameter for describing the test results.

Key words: low-cycle fatigue, multiaxial fatigue, energy approach, lifetime, high temperature

Notations

E	– Young's modulus
k	– strain ratio ($k = \varepsilon_3/\varepsilon_1$ or $k = \varepsilon_{xx}/\varepsilon_{yy}$)
K', n'	– cyclic strain hardening coefficient and exponent
l_η, m_η, n_η	– direction cosines of unit vector $\boldsymbol{\eta}$ against coordinates (x, y, z)
N_f	– number of cycles to failure

s_{ij}	–	components of stress tensor deviator
$W_{a\eta}$	–	amplitude of strain energy density in critical plane with normal vector $\boldsymbol{\eta}$
$W_{a\eta\varepsilon}$	–	amplitude of strain energy density in critical plane when stress has been calculated from measured strain
$W_{a\eta\sigma}$	–	amplitude of strain energy density in critical plane when strain has been calculated from measured stress
x, y, z	–	spatial coordinates of specimen
α	–	angle between vector normal to critical plane $\boldsymbol{\eta}$ and the x axis
δ_{ij}	–	Kronecker delta
$\Delta\sigma_{\eta}, \Delta\varepsilon_{\eta}$	–	normal stress and strain ranges in $\boldsymbol{\eta}$ direction
$\varepsilon_1, \varepsilon_2, \varepsilon_3$	–	principal strains
$\varepsilon_{ij}(i, j = x, y, z)$	–	strain tensor components ($\gamma_{ij} = 2\varepsilon_{ij}, i \neq j$)
ε'_f, c	–	fatigue ductility coefficient and exponent
ε_{eq}^p	–	equivalent plastic strain
$\boldsymbol{\eta}$	–	unit vector normal to critical plane
ν	–	Poisson's ratio
γ	–	engineering shear strain
$\sigma_1, \sigma_2, \sigma_3$	–	principal stresses
$\sigma_{a\eta}, \varepsilon_{a\eta}$	–	normal stress and strain amplitudes in $\boldsymbol{\eta}$ direction
σ_{ij}	–	stress tensor components
σ_{kk}	–	sum of normal stresses ($\sigma_{kk} = \sigma_{xx} + \sigma_{yy} + \sigma_{zz}$)
σ_{eq}	–	equivalent stress
σ'_f, b	–	fatigue strength coefficient and exponent

Subscripts

a	–	amplitude	exp	–	experimental
cal	–	calculation	p	–	plastic
e	–	elastic	t	–	total

1. Introduction

The oldest models of multiaxial fatigue were based on stress. Later, the models using strain were introduced in order to calculate the fatigue life in high- and low-cycle regimes. However, both models have a limited range of application and they cannot be used in some situations. Thus, new models are still being sought. For about thirty years, the energy approach to multiaxial

fatigue has been developed. Recently, some very successful experimental data descriptions and useful algorithms for fatigue life estimation have been proposed. In these algorithms the multiaxial fatigue criteria play the most important role.

The strain energy criteria used for multiaxial fatigue failure can be classified into three groups depending on the type of strain energy density per cycle as a damage parameter (Andrews and Brown, 1989; Curioni and Freddi, 1991; Ellyin, 1974, 1989; Ellyin and Gołoś, 1988; Garud, 1981; Glinka *et al.*, 1995; Gołoś, 1988; Gołoś and Osiński, 1994; Lefebvre *et al.*, 1988; Leis, 1977; Macha, 1979; Nitta *et al.*, 1989). They are:

- criteria based on elastic strain energy density for high-cycle fatigue (HCF),
- criteria based on plastic strain energy density for low-cycle fatigue (LCF),
- criteria based on the sum of plastic and elastic strain energy densities for both low- and high-cycle fatigue (LCF and HCF).

However, the criteria including strain energy density in fracture planes or critical planes are a dominating parameter for describing multiaxial fatigue, and they seem to be most promising.

Ellyin (1974) was the first to propose an energy approach to multiaxial fatigue. His approach includes not only the elastic strain energy density (as generalised Huber-Mises-Hencky hypothesis or Beltrami hypothesis) but also the plastic strain energy density. The Ellyin's parameter is understood as an elastic and plastic strain energy in octahedral planes for HCF and LCF. For HCF, Macha (1979) proposed elastic shear strain energy density in the maximum shear stress plane. Garud's proposal (1981) concerns the sum of plastic strain energy density for all strain components in a cycle under proportional and non-proportional loading for LCF. However, the in- and out-of-phase tension-torsion experimental results verified that the sum of plastic normal and shear strain energy densities in the critical plane is a parameter strongly influencing the fatigue life.

Socie (1987) successfully used the Smith-Watson-Topper parameter (SWT) (Smith *et al.*, 1970), i.e. the normal elastic and plastic strain energy densities in the plane where the maximum normal strain range occurs in proportional and non-proportional tension-torsion HCF and LCF for SUS304 at room temperature.

Lefebvre *et al.* (1988) used the plastic effective strain energy density in a cycle as a LCF damage parameter. This parameter is equivalent to the shear strain energy in the octahedral plane.

Nitta *et al.* (1989) applied the energy fatigue parameters related with the fracture plane by analysing the experimental results in tension-torsion proportional and non-proportional HCF and LCF. They proposed:

- elastic and plastic normal strain energy densities in the maximum normal strain range plane,
- elastic and plastic shear strain energy densities in the maximum shear strain range plane,
- non-linear sum of the two above energies in the fracture plane.

These parameters depend on the strain ratio, phase differences and fracture mode.

Hoffman and Seeger (1989) proposed the modified SWT parameters for proportional HCF and LCF. The authors suggested that the fatigue damage parameter should be the elastic and plastic normal strain energy in the maximum normal strain plane or the elastic and plastic shear strain energy in the maximum shear strain plane. The choice of either the former or latter depends on the material property.

Chu *et al.* (1993) proposed the sum of elastic and plastic strain energy densities of normal and shear components in the critical plane (for the maximum sum of both energies) for proportional and non-proportional HCF and LCF. For the same loading, Liu (1993) proposed a sum of the elastic and plastic energy densities of normal and shear strains (virtual strain energy, VSE parameter) in the critical plane. The plane is determined by seeking the maximum value of one energy component, according to Mode I or Mode II. Chen *et al.* (1999) also used VSE parameter for proportional and non-proportional LCF in the critical planes of maximum normal strain or maximum shear strain. For proportional HCF and LCF, Glinka *et al.* (1995) used a sum of the elastic and plastic strain energy densities of the normal and shear components in the maximum shear strain plane. The parameter proposed by Glinka *et al.* has been recently modified and extended to non-proportional loading by Pan *et al.* (1999).

An energy based critical plane approach was proposed by Rolovic and Tipton (1999), Varvani-Farahani and Topper (2000), Park and Nelson (2000), and Jiang (2000) to multiaxial cycle fatigue and to multiaxial random fatigue by Łagoda (2001), Łagoda and Macha (2000, 2001), Łagoda *et al.* (1999). An extensive review of energy-based criteria of multiaxial fatigue failure has been published by Macha and Sonsino (1999).

From the above papers, the proposed energy models have two aspects; the definition of strain energy density and the introduction of the critical plane. It should be emphasised that there exists no universal critical plane

applicable to widely varied multiaxial stress states (Łagoda, 2001; Łagoda and Macha, 2000, 2001; Łagoda *et al.*, 1999). The experimental verification of the proposed energy models is still a scientific open question. Many experimental data should be obtained in order to prove the validity of these models for various materials, loading conditions, temperature and so on.

The objective of this paper is to examine the strain energy density parameter by applying the parameter to the proportional LCF data using SUS304 stainless steel hollow cylinder and cruciform specimens at elevated temperatures.

For the case of SUS 304 steel in tension-torsion LCF of cylindrical specimens, Socie (1987), and Nitta *et al.* (1989) showed that the normal strain energy density in the critical plane of the maximum normal strain range was a suitable parameter at room temperature and 1096 K, respectively.

The authors will examine the suitability of the energy parameter for describing the tension-torsion and biaxial tension LCF behaviour of SUS304 steel at 923 K. The energy parameter considered in the paper is also based on the SWT idea (Smith *et al.*, 1970) but it uses a newly defined critical plane. In Łagoda (2001), Łagoda and Macha (2000, 2001), Łagoda *et al.* (1999) it has been shown that the normal strain energy density in the critical plane (the plane of the maximum damage) may be successfully used for evaluation of the fatigue life of 10HNAP steel under random biaxial tension of cruciform specimens and tension-compression with torsion for 35NCD16 steel and GGG40 and GGG60 cast irons. This parameter will be subjected to another assessment using two series of data for SUS304 steel.

2. Fatigue tests

The test material used was SUS 304 stainless steel of which the chemical composition is presented in Table 1. This paper analysed two fatigue data sets. One is the tension-torsion LCF data using hollow cylinder specimens shown in Fig. 1 in the principal strain ratio range of $-1 \leq k \leq 0.5$ (Sakane *et al.*, 1987) and the other is the tension-tension LCF data using cruciform specimens shown in Fig. 2 in the normal strain ratio range of $-1 \leq k \leq -1$ (Itoh *et al.*, 1994). The experiments were done in loading phase. The strain wave used was a fully reversed triangular strain wave with the Mises equivalent strain rate of 0.1%/s at 923 K.

Table 1. Chemical composition of SUS304 steel in weight percent ratio

C	Mn	Si	P	S	Cr	Ni	Fe
0.06	1.13	0.38	0.008	0.021	18.52	8.74	bal.

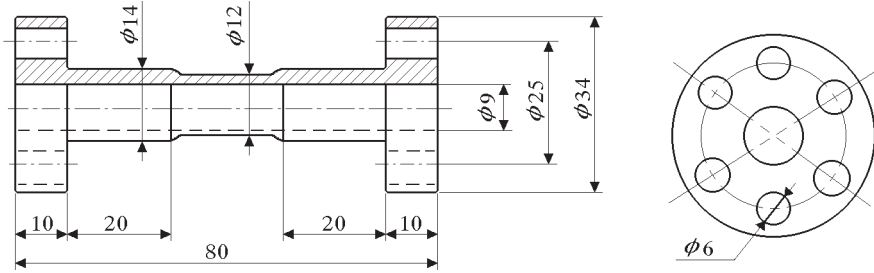


Fig. 1. Cylinder specimen

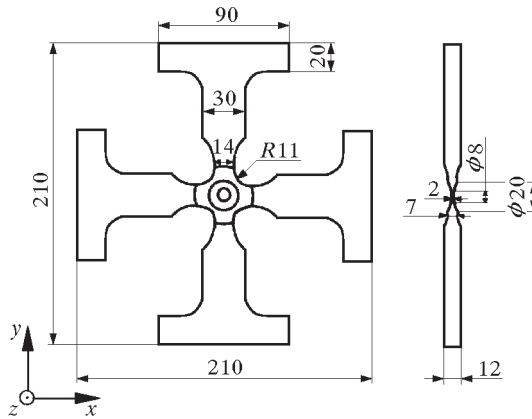


Fig. 2. Cruciform specimen

Tables 2 and 3 summarize the experimental results in tension-torsion and tension-tension data, respectively. Graphical representations of these results are shown in Fig.3 and Fig.4. The value of Young's modulus was assumed (Itoh *et al.*, 1994; Sakane *et al.*, 1987) to be 158 GPa and that of Poisson's ratio 0.3 in the following analysis. The relationship between the strain ranges and cycles to failure in the uniaxial stress state was approximated by the following equation according to the ASTM method (Socie, 1987)

$$\varepsilon_a = \varepsilon_{ae} + \varepsilon_{ap} = \frac{\sigma'_f}{E}(2N_f)^b + \varepsilon'_f(2N_f)^c \quad (2.1)$$

Table 2. Fatigue test results for thin-walled cylindrical specimens

$k = \frac{\varepsilon_{a3}}{\varepsilon_{a1}}$	ε_{ayy} [%o]	σ_{ayy} [MPa]	γ_{axy} [%o]	τ_{axy} [MPa]	N_f [cycles]	$W_{a\eta}$ [MJ/m ³]	N_{cal} [cycles]	$W_{a\eta\sigma}$ [MJ/m ³]	$W_{a\eta\varepsilon}$ [MJ/m ³]
-0.50	7.50	319	0	0	200	1.196	185	1.303	1.121
	5.00	246	0	0	720	0.615	718	0.533	0.627
	3.50	219	0	0	1200	0.384	1963	0.365	0.375
	2.50	201	0	0	7600	0.252	5029	0.278	0.226
-0.52	7.25	286	3.35	76	270	1.145	202	1.200	1.106
	4.90	256	2.25	62	820	0.678	586	0.776	0.615
	3.40	213	1.55	56	1480	0.398	1815	0.436	0.369
-0.57	6.50	234	6.50	106	280	1.035	247	0.928	1.061
	4.35	161	4.35	103	1240	0.529	985	0.419	0.598
	3.00	152	3.05	96	3280	0.347	2452	0.339	0.359
-0.64	5.03	229	9.20	112	530	1.020	255	0.947	0.995
	3.55	182	6.15	112	1180	0.581	808	0.595	0.559
	2.50	198	4.30	80	2100	0.391	1887	0.463	0.340
-0.74	3.75	172	11.25	160	510	0.971	281	1.106	0.884
	2.50	140	7.50	147	730	0.559	877	0.984	0.497
	1.75	101	5.25	128	2720	0.315	3039	0.368	0.295
-0.86	1.95	103	12.55	178	1050	0.823	393	0.930	0.744
	1.30	135	8.35	129	1750	0.490	1160	0.502	0.419
	0.90	87	5.85	118	8900*	0.277	4056	0.266	0.253
-1.00	0	9	13.00	191	500	0.635	671	0.746	0.585
	0	24	8.65	157	2000	0.368	2154	0.401	0.335
	0	16	6.05	139	8600	0.225	6527	0.256	0.203

* - no crack

Table 3. Fatigue test results for cruciform specimens

$k = \frac{\varepsilon_{axx}}{\varepsilon_{ayy}}$	ε_{ayy} [%o]	σ_{ayy} [MPa]	σ_{axx} [MPa]	N_f [cycles]	$W_{a\eta}$ [MJ/m ³]	N_{cal} [cycles]
-1	5.0	163	-163	2100	0.408	1720
	3.5	141	-141	6200	0.247	5265
	2.5	122	-122	35000	0.153	16278
	1.5	95*	-95*	> 100000	0.071	115300
-0.5	5.0	251	-21	1100	0.628	687
	3.5	212	-21	3200	0.371	2116
	2.5	181	-22	13500	0.226	6461
	2.0	161*	-22*	> 100000	0.161	14391
	1.5	137*	-21*	> 120000	0.103	43571

0	5.0	310	135	600	0.775	444
	3.5	264	111	2800	0.462	1315
	2.5	224	90	7200	0.280	3959
	2.0	200	79	40000	0.200	8590
	1.5	170	65	80000	0.128	25217
0.5	5.0	329	254	350	0.823	393
	3.5	282	216	700	0.494	1140
	2.5	241	182	4700	0.301	3364
	2.0	216	163	4800	0.216	7176
	1.5	185	138	38000	0.139	20574
1	3.5	287	287	700	0.502	1101
	2.5	247	247	2800	0.300	3389
	2.0	222	222	2200	0.222	6734
	1.5	192	192	10000	0.144	18868

* – no crack

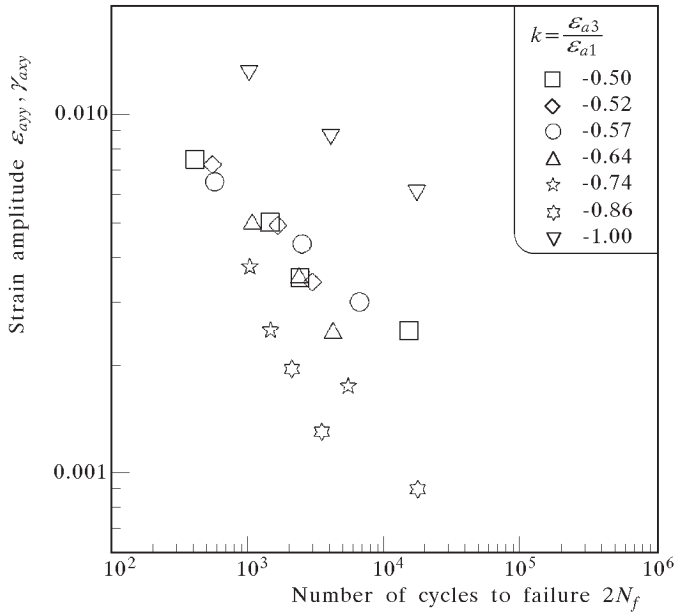


Fig. 3. Fatigue test results using tube specimens under tension-torsion multiaxial stress states

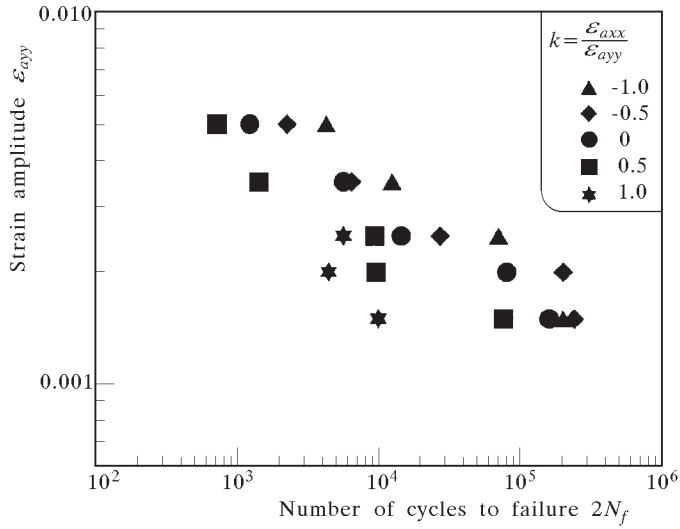


Fig. 4. Fatigue test results using cruciform specimens under biaxial tension-compression multiaxial stress states

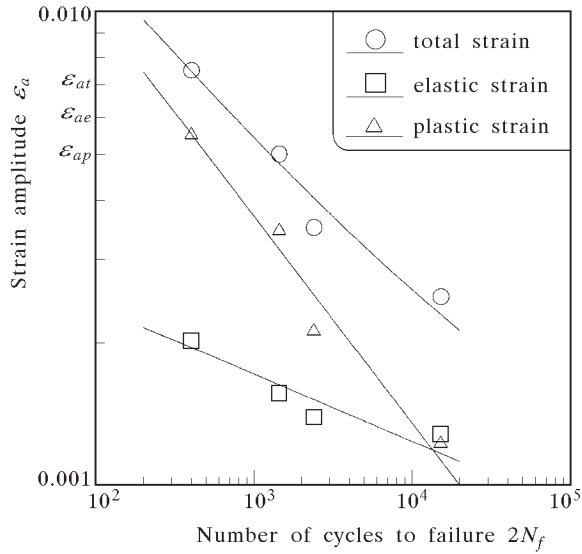


Fig. 5. Correlation of uniaxial tension fatigue lives of tube specimens with total, elastic and plastic strain range

The material constants determined in the low-cycle range (200-7600 cycles) are $\sigma'_f = 722$ MPa, $\varepsilon'_f = 0.075$, $b = -0.42$, $c = -0.436$, (Fig. 5).

The following Ramberg-Osgood model was used to express the cyclic stress-strain curve

$$\varepsilon_a = \varepsilon_{ae} + \varepsilon_{ap} = \frac{\sigma_a}{E} + \left(\frac{\sigma_a}{K'}\right)^{\frac{1}{n'}} \quad (2.2)$$

Comparing the amplitudes of the elastic and plastic strains, ε_{ae} and ε_{ap} , from equations (2.1) and (2.2) we have

$$\frac{\sigma_a}{E} = \frac{\sigma'_f}{E} (2N_f)^b \quad \left(\frac{\sigma_a}{K'}\right)^{\frac{1}{n'}} = \varepsilon'_f (2N_f)^c \quad (2.3)$$

Substituting σ_a in Eq. (2.3)₁ into Eq. (2.3)₂ and slightly modifying, gives

$$\left(\frac{\sigma'_f}{K'}\right)^{\frac{1}{n'}} (2N_f)^{\frac{b}{n'}} = \varepsilon'_f (2N_f)^c \quad (2.4)$$

Since Eq. (2.4) holds for every N_f , we can obtain the two independent equations

$$\left(\frac{\sigma'_f}{K'}\right)^{\frac{1}{n'}} = \varepsilon'_f \quad \frac{b}{n'} = c \quad (2.5)$$

The value of K' is 1680 MPa and that of n' is 0.326, so that

$$K' = \frac{\sigma'_f}{(\varepsilon'_f)^{n'}} = 1680 \text{ MPa} \quad n' = \frac{b}{c} = 0.326 \quad (2.6)$$

3. Mathematical model

For determining the amplitudes of normal stresses in cruciform specimens we used the Hencky total elastic-plastic deformation theory, as suggested by Moftakhar *et al.* (1995)

$$\varepsilon_{ij} = \varepsilon_{ij}^e + \varepsilon_{ij}^p = \frac{1+\nu}{E} \sigma_{ij} - \frac{\nu}{E} \sigma_{kk} \delta_{ij} + \frac{3}{2} \frac{\varepsilon_{eq}^p}{\sigma_{eq}} s_{ij} \quad (3.1)$$

where

$$\sigma_{eq} = \sqrt{\frac{3}{2} s_{ij} s_{ij}} \quad s_{ij} = \sigma_{ij} - \frac{1}{3} \sigma_{kk} \delta_{ij} \quad (3.2)$$

To express the stress-strain relationship in multiaxial proportional loading, the Mises equivalent values were used as follows, where the same K' and n' values in Eq. (2.2) were used

$$\varepsilon_{eq}^p = \left(\frac{\sigma_{eq}}{K'} \right)^{\frac{1}{n'}} \quad (3.3)$$

From Eqs (3.2) and (3.3), the principal strains ε_{a1} , ε_{a2} , ε_{a3} can be written with the principal stresses σ_{a1} , σ_{a2} , σ_{a3} in plane stress conditions as

$$\begin{aligned} \varepsilon_{a1} &= \frac{1}{E}(\sigma_{a1} - \nu\sigma_{a3}) + \frac{1}{2}(K')^{\frac{-1}{n'}}(2\sigma_{a1} - \sigma_{a3})(\sigma_{a1}^2 + \sigma_{a3}^2 - \sigma_{a1}\sigma_{a3})^{\frac{1-n'}{2n'}} \\ \varepsilon_{a2} &= -\frac{\nu}{E}(\sigma_{a1} + \sigma_{a3}) - \frac{1}{2}(K')^{\frac{-1}{n'}}(\sigma_{a1} + \sigma_{a3})(\sigma_{a1}^2 + \sigma_{a3}^2 - \sigma_{a1}\sigma_{a3})^{\frac{1-n'}{2n'}} \\ \varepsilon_{a3} &= \frac{1}{E}(\sigma_{a3} - \nu\sigma_{a1}) + \frac{1}{2}(K')^{\frac{-1}{n'}}(2\sigma_{a3} - \sigma_{a1})(\sigma_{a1}^2 + \sigma_{a3}^2 - \sigma_{a1}\sigma_{a3})^{\frac{1-n'}{2n'}} \end{aligned} \quad (3.4)$$

Since the stresses for the cruciform specimen cannot be directly determined from the applied load, they were determined using Eqs (3.4)_{1,3} and they are listed in Table 3. For the cruciform specimens the calculated stresses $\sigma_3 = \sigma_x$ and $\sigma_1 = \sigma_y$. The z direction stress σ_z was equal to zero, so the strain energy density in the same direction was also equal to zero for the cruciform specimens.

The energy parameter used in this paper includes the maximum elastic and plastic normal strain energy densities in the critical plane. Under proportional loading the amplitude of energy $W_{a\eta}$ in the critical plane with the normal vector $\boldsymbol{\eta}(l_\eta, m_\eta, n_\eta)$ is written as

$$W_{a\eta} = \frac{1}{2}\sigma_{a\eta}\varepsilon_{a\eta} = \frac{1}{8}\Delta\sigma_{a\eta}\Delta\varepsilon_{a\eta} \quad (3.5)$$

where

$$\begin{aligned} \sigma_{a\eta} &= \frac{\Delta\sigma_\eta}{2} = l_\eta^2\sigma_{axx} + m_\eta^2\sigma_{ayy} + n_\eta^2\sigma_{azz} + 2l_\eta m_\eta\tau_{axy} + \\ &+ 2l_\eta n_\eta\tau_{axz} + 2m_\eta n_\eta\tau_{ayz} \\ \varepsilon_{a\eta} &= \frac{\Delta\varepsilon_\eta}{2} = l_\eta^2\varepsilon_{axx} + m_\eta^2\varepsilon_{ayy} + n_\eta^2\varepsilon_{azz} + 2l_\eta m_\eta\varepsilon_{axy} + \\ &+ 2l_\eta n_\eta\varepsilon_{axz} + 2m_\eta n_\eta\varepsilon_{ayz} \end{aligned} \quad (3.6)$$

$\sigma_{a\eta}$ and $\varepsilon_{a\eta}$ are the normal stress and strain amplitudes in direction $\boldsymbol{\eta}$, respectively. (l_η, m_η, n_η) are the direction cosines of $\boldsymbol{\eta}$ against coordinates (x, y, z) .

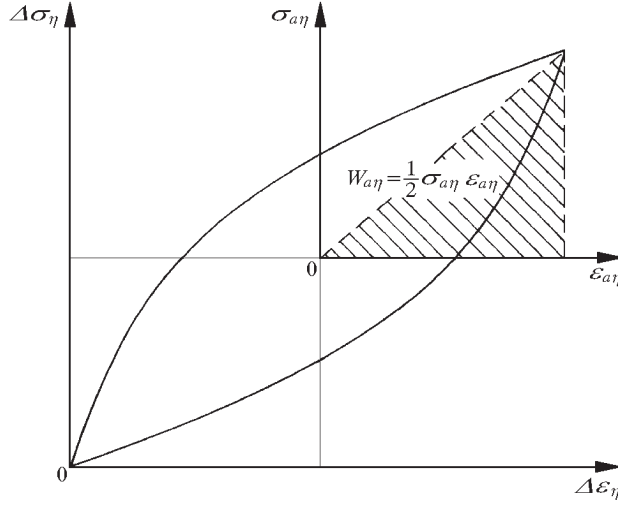


Fig. 6. Graphical interpretation of energy

A graphical presentation of the energy parameter is shown in Fig. 6. In uniaxial tension tests, the strain amplitude-failure cycle ($\varepsilon_a - N_f$) relationship can be rewritten with the strain energy density-failure cycle ($W_a - N_f$) relationship. From Eqs (2.1) and (3.5) we obtain

$$W_a = \frac{1}{2} \sigma_a \varepsilon_a = \frac{\sigma_a}{2} \left[\frac{\sigma'_f}{E} (2N_f)^b + \varepsilon'_f (2N_f)^c \right] \quad (3.7)$$

From (2.3)₁ we have

$$\sigma_a = \sigma'_f (2N_f)^b \quad (3.8)$$

then Eq. (3.7) becomes a new fatigue equation between W_a and N_f

$$W_a = \frac{(\sigma'_f)^2}{2E} (2N_f)^{2b} + \frac{1}{2} \varepsilon'_f \sigma'_f (2N_f)^{b+c} \quad (3.9)$$

4. Algorithm for determination of fatigue lifetime

Figure 7 shows the algorithm for determination of fatigue lifetime using this parameter. At first (stage 1) we measure the strain state components being controlled during the experiments.

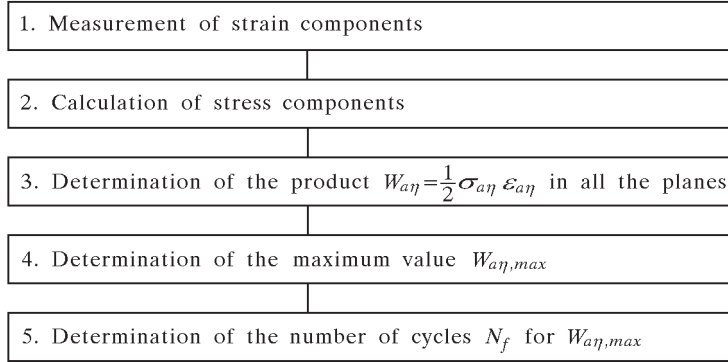


Fig. 7. Algorithm for fatigue lifetime determination

Next (stage 2), we calculate the stress amplitudes. In the case of cylinder specimens it was possible to measure the stress amplitude experimentally, so the experimentally measured stress was used.

Having the stress and strain amplitudes, we can determine the energy amplitude by (3.5) in any plane with the normal vector $\boldsymbol{\eta}$ (stage 3).

The normal stress and strain at any plane can be determined by the following equations for the plane stress conditions from (3.6)

$$\begin{aligned}\sigma_{a\eta} &= l_\eta^2 \sigma_{axx} + m_\eta^2 \sigma_{ayy} + 2l_\eta m_\eta \tau_{axy} \\ \varepsilon_{a\eta} &= l_\eta^2 \varepsilon_{axx} + m_\eta^2 \varepsilon_{ayy} + n_\eta^2 \varepsilon_{azz} + l_\eta m_\eta \gamma_{axy}\end{aligned}\quad (4.1)$$

Note that in the thin-walled cylinder specimen $\sigma_{ayy} = \sigma_{azz} = \tau_{axz} = \tau_{ayz} = \gamma_{axz} = \gamma_{ayz} = 0$ and in the cruciform specimen $\sigma_{azz} = \tau_{axy} = \tau_{axz} = \tau_{ayz} = \gamma_{axy} = \gamma_{axz} = \gamma_{ayz} = 0$.

For a plane stress state, the direction cosines of the vector normal to the critical plane $\boldsymbol{\eta}$ can be described with the angle α between the $\boldsymbol{\eta}$ direction and x axis

$$l_\eta = \cos \alpha \quad m_\eta = \sin \alpha \quad n_\eta = 0 \quad (4.2)$$

The critical plane was searched by the damage cumulation method (Łagoda, 2001; Łagoda and Macha, 2000, 2001; Łagoda *et al.*, 1999; Sakane *et al.*, 1987). The critical plane is the plane which has the maximum energy $W_{a\eta}$ (stage 4). Generally, energy parameter (3.5) agrees with the energy parameter used by Socie (1987) and Nitta *et al.* (1989). The difference concerns only the definition of the critical plane. Socie and Nitta *et al.* assumed the plane with the maximum range of normal strains, and in model (3.5) the critical plane is a

plane with the maximum amplitude of the energy density of normal strains. At our critical plane the accumulated fatigue damage is the maximum according to the assumed fatigue parameter.

It should be also stated that in the case of cruciform specimens under the assumed loading, verified energy parameter (3.5) is the same as that resulting from the criterion proposed by Liu (1993) for thin-walled cylindrical specimens under crack mode I.

At the final step (stage 5), we can calculate a number of cycles to failure, N_f based on Eq. (3.9).

5. Comparison of calculated life time with actual life time

Figure 8 compares the calculated lives with the experimental ones for the cylindrical and cruciform specimens.

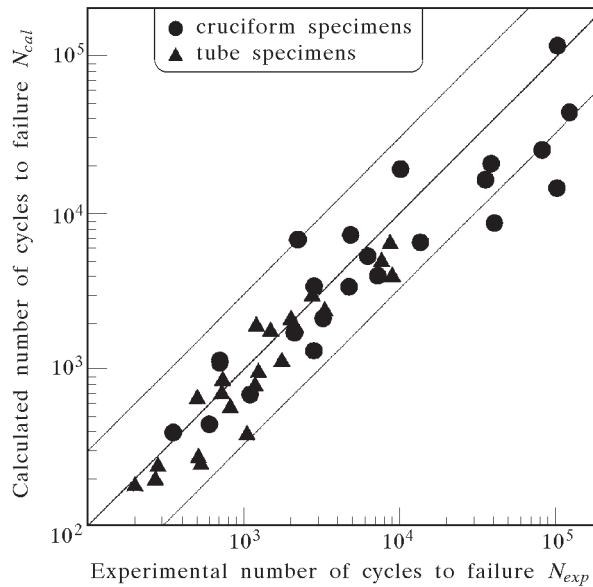


Fig. 8. Comparison of predicted and experimental fatigue lives for cylinder and cruciform specimens

In the figure a factor of 3 scatter band based on the experimental data is presented. For 200-10000 failure cycles, all the results are located within that scatter band. For higher numbers of cycles they are greater, but in both

cases we observe a trend to overestimate the energy amplitude. It is probably because the parameters of curve (2.1) for uniaxial tension-compression have been determined from the tests for a lower number of cycles to failure.

The parameter of plastic and elastic energy of normal strains in the critical plane can be assumed effective for low-cycle fatigue life evaluation for the cylinder and cruciform specimens tested under the biaxial proportional loading at elevated temperature. Since the parameter is effective in the case of correlation of the experimental data obtained for the cruciform specimens of 10HNAP steel under random non-proportional biaxial tension-compression in the range of medium and high numbers of cycles at room temperature (Łagoda, 2001; Łagoda and Macha, 2000, 2001; Łagoda *et al.*, 1999), it should be verified in further tests.

Hencky's constitutive equations (3.1)-(3.4) and the parameters of the cyclic stress-strain curve of Ramberg-Osgood's type are used to determine the stresses on the basis of the given strains. While applying the energy parameter no additional measurements are required to calculate the stresses.

In order to prove that statement we calculated the amplitudes of energy density in the critical planes $W_{a\eta}$ for:

- (a) experimental strains $\varepsilon_{a\eta}$ and $\gamma_{a\eta}$ (Table 2) and stresses determined according to equations (3.1)-(3.4),
- (b) experimental stresses $\sigma_{a\eta}$ and $\tau_{a\eta}$ (Table 2) and strains determined according to equations (3.1)-(3.4).

The correlation shown in Fig. 9 is equated from (3.9) as

$$W_a = 1.65(2N_f)^{-0.284} + 27.075(2N_f)^{-0.578} \quad (5.1)$$

The comparison shows that both calculation methods using Eqs (3.1)-(3.4) are efficient, although the first one (measurement of strains and stress calculation) is more precise.

6. Conclusion

An elastic and plastic strain energy parameter normal to the critical plane was proposed. This parameter can be evaluated from the stress and strain components applied to specimens. If only the strain components are given, the stress components can be calculated by using Hencky's equation.

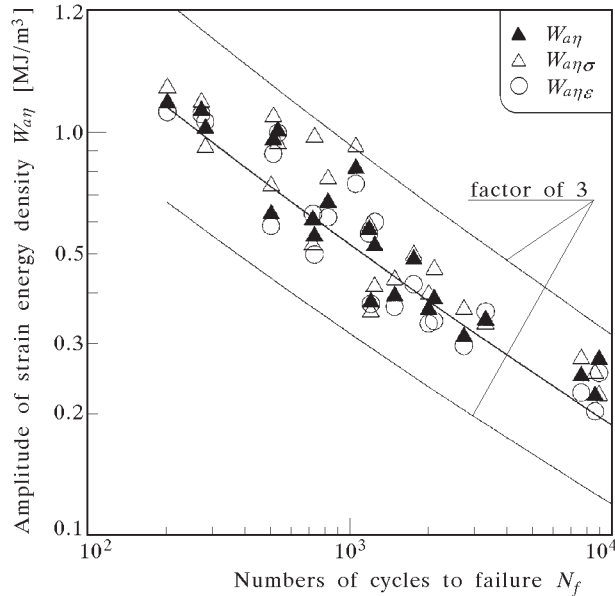


Fig. 9. Correlation of fatigue lives of tube specimens with three energy parameters $W_{a\eta}$, $W_{a\eta\sigma}$ and $W_{a\eta\varepsilon}$

The proposed energy parameter correlated the tension-torsion and biaxial tension low cycle fatigue life of SUS304 steel within a factor of three scatter band. The parameter was proved to be effective for the correlation of multiaxial low cycle fatigue lives in the principal strain range of $-1 \leq k \leq 1$.

Acknowledgements

The paper was realized within the research project 7T07B01818, partly financed by the Polish State Committee for Scientific Research in 2000-2002 and NATO Advanced Fellowships Programme 1|J|2000.

References

1. ANDREWS R.M., BROWN M.W., 1989, Elevated temperature out-of-phase fatigue behaviour of a stainless steel, in: *Biaxial and Multiaxial Fatigue EGF3*, M.W.Brown and K.J. Miller (eds.), MEP, London, 641-658
2. ASTM E 739-80 (1986), Standard practice for: Statistical analysis of linearized stress-life ($S-N$) and strain-life ($\varepsilon-N$) fatigue data, in: *Annual Book of ASTM Standards*, vol. 03.01, Philadelphia, 1989, 667-673

3. CHEN X., XU SH.Y., HUANG D.X., 1999, Critical plane-strain energy density criterion of multiaxial low-cycle fatigue life, *FATIGUE'99, Proc. 7IFC*, Beijing, P.R.China, Eds X.R. Wu and Z.G. Wang, Higher Education Press, II, 959-964
4. CHU C.C, CONLE F.A., BONNEN J.J., 1993, Multiaxial stress-strain modeling and fatigue life prediction of SAE axle shafts, *Advances in Multiaxial Fatigue, ASTM STP, 1191*, D.L. McDowell and R.Ellis, Eds., American Society for Testing and Materials, Philadelphia, 37-54
5. CURIONI S., FREDDI A., 1991, Energy-based torsional low-cycle fatigue analysis, *Fatigue under Biaxial and Multiaxial Loading*, ESIS 10, Eds. K.F.Kussmaul, D.L.McDiarmid, D.F.Socie, MEP, London, 23-33
6. ELLYIN F., 1974, A criterion for fatigue under multiaxial states of stress, *Mechanics Research Communications*, **1**, 4, 219-224
7. ELLYIN F., 1989, Cyclic strain energy as a criterion for multiaxial fatigue failure, in: *Biaxial and Multiaxial Fatigue, EGF3*, K.J. Miller and M.W.Brown (eds.), MEP, London, 571-583
8. ELLYIN F., GOŁOŚ K., 1988, Multiaxial fatigue damage criterion, *Trans. ASME, JEMT*, **110**, 63-68
9. GARUD Y.S., 1981, A new approach to the evaluation of fatigue under multiaxial loadings, *Trans. ASME, JEMT*, **103**, 118-125
10. GLINKA G., SHEN G., PLUMTREE A., 1995, A multiaxial fatigue strain energy density parameter related to the critical fracture plane, *Fatigue Fract. Engng Mater. Struct.*, **18**, 1, 37-64
11. GOŁOŚ K., 1988, An energy based multiaxial fatigue criterion, *Engineering Transactions*, **36**, 1, 55-63
12. GOŁOŚ K.M., OSIŃSKI Z., 1994, Multiaxial fatigue criterion under proportional loading including mean strain effect, *Fourth Int. Conf. on Biaxial/Multiaxial Fatigue*, St Germain en Laye (France), **II**, 303-315
13. HOFFMAN H., SEEGER T., 1989, Stress-strain analysis and life predictions of a notched shaft under multiaxial loading, *Multiaxial Fatigue: Analysis and Experiments, AE-14*, Eds G.E. Leese and D. Socie, Society of Automotive Engineers, Inc., Warrendale, USA, 81-99
14. ITOH T., SAKANE M., OHNAMI M., 1994, High temperature multiaxial low cycle fatigue of cruciform specimen, *Trans. ASME, JEMT*, **116**, 90-98
15. JIANG Y., 2000, A fatigue criterion for general multiaxial loading, *Fatigue Fract. Engng Mater. Struct.*, **23**, 1, 19-32
16. LEFEBVRE D., NEALE K.W., ELLYIN F., 1988, A criterion for low-cycle fatigue failure under biaxial states of stress, *Trans. ASME, JEMT*, **103**, 1-6
17. LEIS B.N., 1977, An energy-based fatigue and creep-fatigue damage parameter, *Trans. ASME, JPVT*, **99**, 524-533

18. LIU K.C., 1993, A method based on virtual strain-energy parameters for multiaxial fatigue life prediction, *Advances in Multiaxial Fatigue, ASTM STP, 1191*, D.L. McDowell and R.Ellis, Eds., American Society for Testing and Materials, Philadelphia, 87-84
19. ŁAGODA T., 2001, Energy models for estimation on fatigue life of materials subjected to uniaxial and multiaxial random loading, *Studies and Monographs, 121*, Technical University of Opole, p.148 (in Polish)
20. ŁAGODA T., MACHA E., 2000, Generalization of energy-based multiaxial fatigue criteria to random loading, *Multiaxial Fatigue and Deformation: Testing and Prediction, ASTM STP, 1387*, S. Kalluri and P.J. Bonacuse, Eds, American Society for Testing and Materials, West Conshohocken, PA, 173-190
21. ŁAGODA T., MACHA E., 2001, Energy approach to fatigue life estimation under combined tension with torsion, *Scientific Papers of the Technical University of Opole, 67*, 269/2001, Opole, Poland, 163-182
22. ŁAGODA T., MACHA E., BĘDKOWSKI W., 1999, A critical plane approach based on energy concepts: application to biaxial random random tension-compression high-cycle fatigue regime, *Int. J. Fatigue, 21*, 431-443
23. ŁAGODA T., MACHA E., NIEŚLONY A., MOREL F., 2001, The energy approach to fatigue life of high strength steel under variable-amplitude tension with torsion, *Proc. of the 6th ICBMFF*, Lisbon, Ed. M. Moreira de Freitas, **I**, 233-240
24. MACHA E., 1979, Mathematical models of the life to fracture for materials subject to random complex stress systems, *Scientific Papers of the Institute of Materials Science and Applied Mechanics of Wrocław Technical University, 41, Monographs, 13*, Wrocław, p.99 (in Polish)
25. MACHA E., SONSINO C.M., 1999, Energy criteria of multiaxial fatigue failure, *Fatigue Fract. Engng. Mater. Struct.*, **22**, 1053-1073
26. MOFTAKHAR A., BUCZYŃSKI A., GLINKA G., 1995, Calculation of elasto-plastic strains and stresses in notches under multiaxial loading, *International Journal of Fracture, 70*, 357-373
27. NITTA A., OGATA T., KUWABARA K., 1989, Fracture mechanisms and life assessment under high-strain biaxial cyclic loading of type 304 stainless steel, *Fatigue Fract. Engng. Mater. Struct.*, **12**, 2, 77-92
28. PAN W.-F., HUNG C.-Y., CHEN L.-L., 1999, Fatigue life estimation under multiaxial loadings, *Int. J. Fatigue, 21*, 3-10
29. PARK J., NELSON D., 2000, Evaluation of an energy-based approach and a critical plane approach for predicting constant amplitude multiaxial fatigue life, *Int. J. Fatigue, 22*, 23-39

30. ROLOVIC R., TIPTON S.M., 1999, An energy based critical plane approach to multiaxial fatigue analysis, in: *Fatigue and Fracture Mechanics*, **XXIX**, *ASTM STP*, **1332**, T.L. Panontin and S.D. Sheppard, Eds., American Society for Testing and Materials, West Conshohocken, PA, 599-613
31. SAKANE M., OHNAMI M., SAWADA M., 1987, Fracture modes and low-cycle biaxial fatigue life at elevated temperature, *Trans. ASME, JEMT*, **109**, 236-243
32. SMITH K.N., WATSON P., TOPPER T.H., 1970, A stress-strain function for the fatigue of metals, *Journal of Materials*, **5**, 4, 767-776
33. SOCIE D.F., 1987, Multiaxial fatigue damage models, *Trans. ASME JEMT*, **109**, 293-298
34. VARVANI-FARAHANI A., TOPPER T.H., 2000, A new multiaxial fatigue life and crack growth rate model for various in-phase and out-of-phase strain paths, *Multiaxial Fatigue and Deformation: Testing and Prediction*, *ASTM STP*, **1387**, S. Kalluri and P.J. Bonacuse, Eds., American Society for Testing and Materials, West Conshohocken, PA, 305-322

Ocena wysokotemperaturowej trwałości zmęczeniowej stali SUS304 za pomocą parametru energetycznego w płaszczyźnie krytycznej

Streszczenie

Praca dotyczy zastosowania parametru energetycznego, sumy gęstości energii sprężystej i plastycznej odkształcenia w płaszczyźnie krytycznej do korelacji dwóch serii proporcjonalnych, dwuosiowych, niskocyklowych trwałości zmęczeniowych stali nierdzewnej SUS303 w podwyższonej temperaturze. Badano cienkościenne próbki cylindryczne poddane siedmiu proporcjonalnym torom odkształcenia w warunkach kombinacji rozciągania-skręcania oraz próbki krzyżowe poddane pięciu proporcjonalnym torom odkształcenia w warunkach dwuosiowego rozciągania-ściskania. Badania prowadzono w temperaturze 923 K. Gęstość energii całkowitego odkształcenia normalnego w płaszczyźnie maksymalnego uszkodzenia była odpowiednim parametrem do opisanía wyników badań.

Manuscript received March 20, 2002; accepted for print August 14, 2002